

Influence of milling process parameters and significance of tools to improve the surface quality of GFRP composites

I. S. N. V. R. Prasanth, D. V. Ravishankar, M. Manzoor Hussain & Chandra Mouli Badiganti

To cite this article: I. S. N. V. R. Prasanth, D. V. Ravishankar, M. Manzoor Hussain & Chandra Mouli Badiganti (2022) Influence of milling process parameters and significance of tools to improve the surface quality of GFRP composites, *Machining Science and Technology*, 26:1, 120-136, DOI: [10.1080/10910344.2021.1998830](https://doi.org/10.1080/10910344.2021.1998830)

To link to this article: <https://doi.org/10.1080/10910344.2021.1998830>



Published online: 02 Dec 2021.



Submit your article to this journal [↗](#)



Article views: 38




View related articles [↗](#)



View Crossmark data [↗](#)



Influence of milling process parameters and significance of tools to improve the surface quality of GFRP composites

I. S. N. V. R. Prasanth^a, D. V. Ravishankar^b, M. Manzoor Hussain^c, and Chandra Mouli Badiganti^d 

^aDepartment of Mechanical Engineering, Malla Reddy Engineering College, Hyderabad, India; ^bDepartment of Mechanical Engineering, TKR College of Engineering & Technology, Hyderabad, India; ^cDepartment of Mechanical Engineering, JNTUH, Hyderabad, India; ^dDepartment of Mechanical Engineering, RISE Krishna Sai Prakasam Group of Institutions, Ongole, India

ABSTRACT

The anisotropic nature of polymer composites presents many challenges for manufacturers to adopt appropriate machining processes. In the present investigation, end milling experiments were conducted on glass fiber reinforced polymer laminates with five varieties of customized cutting tools with different angles of rake and clearance. The performance of the tools was evaluated in terms of their machining force, surface roughness and delamination factor at spindle speeds in the range of 690–2500 rpm. From the observations, relatively high rake and angled clearance tools performed better than the rest of the tools under consideration in terms of delamination and machined surface finishing. The milling operations performed at a spindle speed of 1950 rpm produced better surface quality. Observations from SEM graphs, exposed surface defects due to milling, generated at lower spindle speeds of 690 rpm and at higher spindle speeds of 2500 rpm with the tool signature of low angle rake and angled clearance tools out of all five tools considered for the experiments.

KEYWORDS

Bi-directional glass fiber reinforced polymers; conventional milling; customized carbide tipped tools; surface integrity; SEM

Introduction

Manufacturing techniques commonly used in glass fiber reinforced polymer (GFRP) composites do not require much machining to manufacture a finished product other than trimming and finishing. However, in special cases such as large pipeline fittings and aircraft parts, the milling and drilling of the components cannot be eliminated. As well as end milling is also used in the development of fiber reinforced polymer (FRP) molding tooling systems. Machining is inevitable in special situations where riveted holes and slots are used for mating one component (composite) with others

(traditional isotropic material). Machining operations, such as turning, drilling, milling and trimming operations, have traditionally been used to make keyholes (Lopresto et al., 2016). Abrão et al. (2007) has observed that maintaining closer dimensional accuracy is necessary in assembly of parts to obtain a high degree of geometrical tolerance and surface finish. In wide and relatively dense composite parts, milling is carried out extensively, especially in jet engine casings, wind turbine blades, racing car bodies and marine hulls (An et al., 2021; Azmi et al., 2012). In machining the reinforcements, orientations may be disturbed due to abnormal cutting reaction forces. Zhang et al. (2001) has found fiber-matrix de-bonding takes place at a depth of cut range between 0.125 and 0.25 mm.

The current study examines ways to minimize damages to machined surface, focusing on FRP composites. Thus, understanding the machinability characterization and mechanism of machining of GFRP composites is an important research area in the field of secondary manufacturing. Cai et al. (2019) investigated precision machining mechanism in orthogonal cutting of carbon fiber reinforced polymer (CFRP) materials. An optimum cutting speed of 200 mm/min and small depth of cut 20 μm were recommended to achieve lower machining force and better surface finish. An et al. (2015) carried out orthogonal machining operations with five varieties of cutting tools (with different tool rake and clearance angle). Results showed large rake angle tool (25°) helps to ease separation of chips from machining surface, considerably reducing machining force. Additionally, use of larger rake angle produces defect-free machining surface. Cutting responses of CFRP materials is investigated (An et al., 2019; An et al., 2020). Can (2019) reported performance of four varieties of end milling tools on sheet mold compound (SMC) composites. Taguchi L16 OA experiments were conducted and repeated thrice. Latha et al. (2011) has modeled and performed optimization using Taguchi Method on a GFRP composite for various process parameters. Optimization of GFRP during drilling process and the effect of deamination factor by the process parameters is performed and found that feed rate influences the most in the delamination (Srinivasan et al., 2017).

Slamani et al. (2019) also reported on the effect of cutting process parameters in edge trimming of CFRP composites on machined surface quality. Researchers have used condensation vapor deposition diamond coated tool to examine surface integrity and tool wear. Better results (namely minimized delamination) were seen at lower feed rates and higher spindle speeds. Previous researchers (Wang et al., 1995; Calzada et al., 2012; Slamani et al., 2015) found machining forces were affected by few input factors, such as machining process conditions, properties of cutting tool and tool nomenclature. Chatelain and Zaghbani (2012) reported on

the influence of tool nomenclature on machining force, surface roughness and damage mechanism in trimming of CFRP materials. The experiments were carried out with three carbide Chemical vapor deposition (CVD) coating tools having varieties of tool angles under different machining conditions. They found surface quality was poor when axial cutting forces were high. Study on hole quality of a fiber metal composite is conducted during dry drilling by varying the parameters and coating on the tool (Giasin et al., 2019). Effect of machining parameters in abrasive water jet machining of carbon glass fiber hybrid composite is studied and a mathematical relationship was also developed to validate the results (Ming et al., 2018). Palanikumar (2007) has modeled the surface roughness through response surface method of a GFRP composites and ANOVA is used to validate the results obtained in his study.

Arola et al. (1996) and Ramulu (1997) undertook orthogonal machining studies using Physical vapor deposition (PVD) coated tools on Bi-Directional and Uni-Directional CRRP composites having different fiber ply orientations. The authors found cutting mechanism was highly dependent on type of fiber used while tool geometry and machining conditions had less impact. Arola and Ramulu (1997) studied the effect of slot milling operations on UD-GFRP composites. The authors found cutting force was influenced by fiber angle and chip thickness followed by other machining process parameters (spindle speed and feed rate). Cutting forces were increased from 0° to 90° and then decreased from 90° to 180° while chip thickness was increased.

Arola et al. (1996) and Arola and Ramulu (1997) investigated chip formation mechanism in orthogonal cutting of CFRP composites with varied tool rake and clearance angles, tool materials, and various combination of cutting process parameters. They found chip formation mechanism was affected by direction of cutting tool on work piece angles followed by machining process parameters. Shojaeefard et al. (2019) used Taguchi DOE 4 \times 4 to optimize machining process parameters and avoid surface roughness in machining of sheet metal using 3 helical forming tools. They found surface quality was proportionate to quality and cost. They noted larger diameters of tool provided lower surface roughness and that had no definite effect on other process parameters (cutting speed and feed rate). Findings showed machined damages were influenced by change of fiber arrangement in UD-GFRP composites (Iliescu et al. 2010; Calzada et al. 2012; Jahromi et al. 2014). Optimization of milling process parameters of GFRP composites is carried out by author in his earlier study (Prasanth et al., 2018; Prashanth et al., 2018).

Studies, hence, indicate a poor understanding of tool performance on machined surface damage. This study therefore addresses by examining five

Table 1. Physical properties of GFRP composite constituents.

Type	Density (g/cm ³)	Tensile strength (GPa)	Young's modulus (GPa)
E-glass	2.58	1.75	72.3
Polyester resin	1.2	0.055	2.4

varieties of customized tools to understand surface integrity. In the present research work, the objective is to develop special purpose tools to be adapted to the milling of FRP composite materials to achieve a better milled surface. Further investigations in these directions could lead to the establishment of ISO standards. Existing conventional tools have limitations on tool signature variations. The improvement in clearance angles contributes to a hypothesized reduction in friction between the milling surface and the cutting edge in the current competition. The increase in the angle of the rake also provides the space for the reinforcement to be easily cut, which even contributes to a reduction of the cutting power. The tool signature of the customized tool rake angle is therefore increased by 5° and the clearance angle by 2°. Five types of customized tools were considered for experimentation, i.e., tool-1 rake angle was 15° and its clearance angle 6°; tool-2 rake angle 20° and its clearance angle 8°; tool-3 rake angle 25° and its clearance angle 10°; tool-4 rake angle 30° and its clearance angle 12° and tool-5 rake angle 35° and its clearance angle 14°.

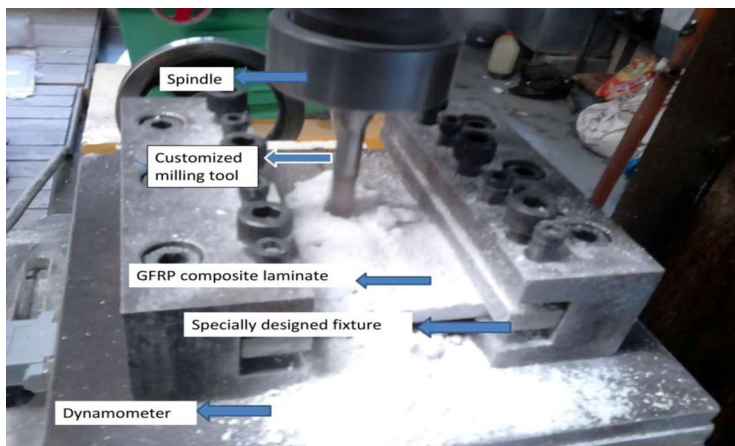
Experimental set up and procedure

In the present investigation, woven roving glass fiber (450GSM and diameter of fiber 25 μm) supplied by Saint Gobain is used. Matrix material used for fabrication of composite laminate is general purpose polyester resin and the hardener used with the combination of catalyst (methyl ethyl ketone peroxide) and cobalt naphthalene as accelerator purchased from local vendor. The polymer laminates were fabricated using hand layup compression molding technique and glass fiber is considered in Bi-Direction [0°/90°]₁₀. A mixture of polyester resin (matrix) and hardener taken in the ratio of 10:1 and stirred in a glass mug and ready mixture is poured into the mold of E-Glass preform under the pressure of 200 kgf. Resin was cured for 5 hours to form a composite laminate. Physical properties of GFRP composite constituents are represented in Table 1.

Work pieces of 100 × 100 × 10 mm blocks were cut using diamond abrasive wheel cutter for milling operations. Burn-off tests were conducted to discover the fiber volume fraction (55%) of experimental GFRP work pieces as per ASTM D2584-68. Mechanical properties (tensile and flexural strength tests) of glass composite laminates are tests on a universal testing machine and the investigation is carried out as per the ASTM D790 and ASTM D 638 standards and tabulated in Table 2. Acid digestion test has

Table 2. Mechanical Properties of GFRP composite laminate.

Tensile test results for GFRP composite laminate				
Sample name	Thickness (mm)	Ultimate tensile load (KN)		Ultimate tensile strength (N/mm ²)
Bi-directional Woven roving composite laminate	5.88	8.59		180
Flexural test results for GFRP composite laminate				
Specimen name	Force (Kgf)	Deflection (mm)	Flexural strength (N/mm ²)	Flexural modulus (N/mm ²)
Bi-directional Woven roving composite laminate	2	0.01	264.5	65690






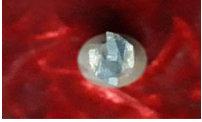



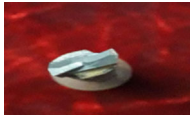
**Figure 1.** Experimental set up for performing milling operations on GFRP composite laminates.

been performed as per ASTM D3171-99, to know the void content in GFRP composite laminate and voids were found to be in the range of 4%–5%.

End milling operations were conducted using conventional universal milling machine to produce work piece slots as shown in Figure 1 (Prasanth et al. 2017b). Five varieties of customized carbide tipped end milling tools of 10 mm diameter were selected and tool specifications are presented in Table 3: tool-1 rake angle was 15°, and its clearance angle was 6°; tool-2 rake angle was 20°, and its clearance angle was 8°; and tool-3 rake angle was 25°, and its clearance angle was 10°, tool-4 rake angle was 30°, and its clearance angle was 12°, and tool-5 rake angle was 35°, and its clearance angle was 14° (see Figure 2). Five spindle speeds were selected: 690, 960, 1153, 1950 and 2500 rpm, and constant feed rate were 120 mm/min while depth of cut was 3 mm.

Machining forces were considered in the direction of tool travel using three axis strain gauge type milling tool dynamometer. Computerized data acquisition system was also used. The work pieces were centrally fixed on the special purpose fixture over the milling tool dynamometer to avoid

Table 3. Tool specifications.

Cutting tool	Diameter in 'mm'	Number of cutting edges	Rake angle	Clearance angle	Cutting tool over view	Cutting edge view of the tool
Customized carbide tipped tool-1	10	2	15°	6°		
Customized carbide tipped tool-2	10	2	20°	8°		
Customized carbide tipped tool-3	10	2	25°	10°		
Customized carbide tipped tool-4	10	2	30°	12°		
Customized carbide tipped tool-5	10	2	35°	14°		

**Figure 2.** Five varieties of customized carbide tipped tools.

machining vibrations. Cutting component forces were recorded as per Langari et al. (2016).

There was customized strain gauge type dynamometer to determine cutting forces during milling. The cutting tool was fed over work piece in x-

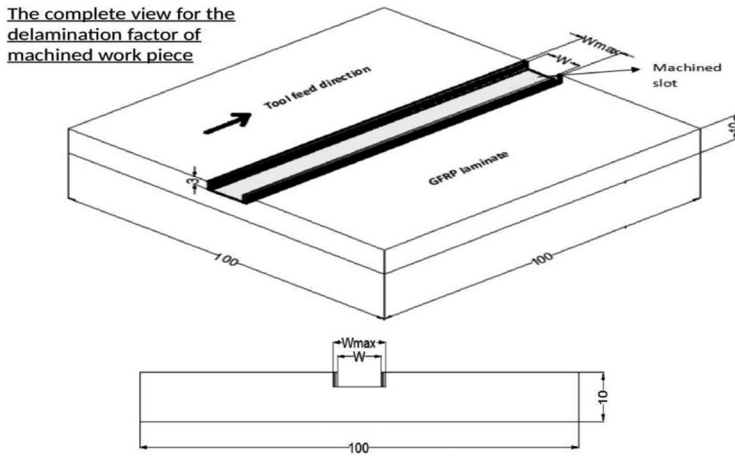


Figure 3. The complete view of delamination factor.

direction (F_x -feed force), F_y -cutting force and F_z -thrust force. The resultant force ' F_R ' was considered as machining force $F_m = \sqrt{F_x^2 + F_y^2 + F_z^2}$. The data analogue device was connected to milling tool dynamometer and output readings were displayed on personal laptop.

Mitutoyo taly surf test (Make-Japan-Model-SJ210) with diamond stylus tip was used to measure surface roughness using center line average method. The surface of machined slot was cleaned so it was free from abrasive particles. To ensure accurate readings, the device was set at 2.5 mm transverse length and 0.8 mm cutoff value. The stylus was kept in contact with the grooved surface to avoid skidding. The surface roughness (R_a) values were measured at three different places and the readings displayed on the screen.

The machined slot widths at three different places were measured using a traveling microscope (Model RVM-201) with an accuracy of $10 \mu\text{m}$. To determine the value of W_{Max} , first, the vernier scale (traveling microscope) was counted as 0.01 mm. These values are substituted in Equation (1). Delamination factor (F_D) was calculated by taking the average value as per Davim and Reis (2005).

Delamination was measured using traveling microscope. Delamination factor (F_D) was determined based on the formulae,

$$F_D = W_{\text{Max}}/W \quad (1)$$

Where W_{Max} = width of the slot after machining in millimeters and W = actual width of slot in millimeters. The complete detail of delamination factor specimen is shown in Figure 3 (Prasanth et al. 2017a). The measurable outcomes in this experiment were F_m , R_a , and F_D as well as surface topology. The machining conditions are shown in Table 4.

Table 4. Experimental plan for milling.

Trial number	Spindle speed in 'rpm'	Tool type	Feed rate in 'mm/min'	Depth of cut in 'mm'	
1 to 5	690	1/2/3/4/5	120	3	
6 to 10	960	1/2/3/4/5	120	3	
11 to 15	1153	1/2/3/4/5	120	3	
16 to 20	1950	1/2/3/4/5	120	3	
21 to 25	2500	1/2/3/4/5	120	3	
Experiment number	Trial number	Spindle speed in 'rpm'	Tool type	Feed rate in 'mm/min'	Depth of cut in 'mm'
1	1	690	1	120	3
	2	960	1	120	3
	3	1153	1	120	3
	4	1950	1	120	3
	5	2500	1	120	3

Four sets of experiments conducted at spindle speeds of 960, 1153, 1950 and 2500 rpm with four tools.

Table 5. Experimental results.

Spindle speed 'N' in 'rpm'	Machining force 'F _m ' in N					Surface roughness 'Ra' in Microns					Delamination Factor 'F _D ' in mm/mm				
	Tool 1	Tool 2	Tool 3	Tool 4	Tool 5	Tool 1	Tool 2	Tool 3	Tool 4	Tool 5	Tool 1	Tool 2	Tool 3	Tool 4	Tool 5
690	30	27.8	28.2	28	26.5	3.61	3.52	3.3	3.23	2.9	1.28	1.26	1.27	1.23	1.2
960	30.8	28.1	28.4	28.2	27.1	3.55	3.4	3.25	3.19	2.7	1.25	1.24	1.23	1.2	1.16
1153	31.5	28.6	30.1	29.3	27.5	3.46	3.25	3.2	3.15	2.54	1.21	1.2	1.17	1.15	1.12
1950	32.8	30.2	30	30.1	28.2	3.4	3.1	3	2.8	2.41	1.18	1.18	1.15	1.13	1.1
2500	34.1	32.1	30.5	30.8	28.8	3.5	3.21	3.22	3	2.49	1.27	1.26	1.25	1.2	1.14

Results and discussion

Obtaining the desired machined surface quality is a major issue in milling of GFRP composites. Hence, choosing suitable machining process parameters is important to obtain better surface finish with minimal surface damages. It must be emphasized machined surface quality of polymer matrix composites depends on spindle speed and tool rake angle.

Machining effects on surface roughness

The effect of type of tool on surface roughness is evaluated using five end milling tools with varied geometries and other machining conditions as shown in Table 4. The results of the experiments are shown in Table 5. Figure 4a shows the effect of spindle speed on surface roughness with five different end milling tools.

The effect of spindle speed on surface roughness is described in two stages. The experiments are shown in Table 4 (trials from 1 to 20) while their results are displayed in Table 5. Spindle speed was increased from 690 to 1950 rpm and surface roughness was decreased continuously from 3.61 to 2.47 μm . Surface roughness became smoother at higher spindle speeds. These desirable spindle speeds are sufficient for material deformation,

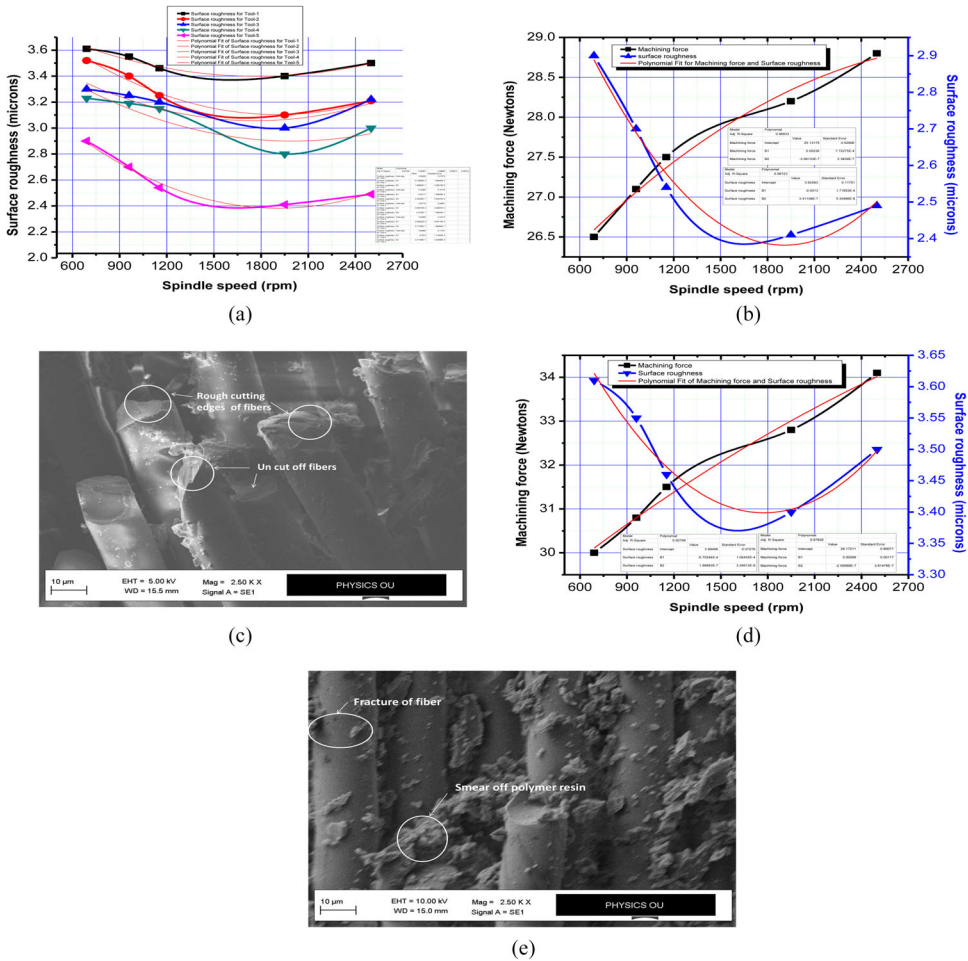


Figure 4. (a) Spindle speed versus roughness with five tools. (b) The interaction effect of machining force and surface roughness at five spindle speeds with tool-5. (c) SEM image for machined surface damages of GFRP laminate, when milling with tool-1 at a spindle speed of 960 rpm. (d) The interaction effect of machining force and surface roughness at five spindle speeds with tool-1. (e) SEM image for machined surface damages of GFRP laminate, when milling with tool-1 at a spindle speed of 2500 rpm.

namely, to form a cutting chip. There was easy withdrawal of chips from milled slot and cutting mechanism was uncomplicated.

The interaction effect between machining force and surface roughness at five different spindle speeds when milling with tool-5 is shown in Figure 4b. Among the five end milling tools, type-5 tool provided the smoothest surface finish at spindle speeds of 1950 rpm with sufficient machining forces (28.2 N). It carried away the chips from the milling surface. Larger tool rake angle held up the fiber shear failures to some extent. There was also less friction between rake face and work piece. Hence, reasonably

better surface roughness ($2.41\ \mu\text{m}$) and an attractive surface finish were obtained.

Table 4 (trial number 1–15) and Table 5 show the experiments and results, respectively. At lower parametric conditions i.e., lower spindle speeds between 690 and 1153 rpm and low rake and clearance angled tool produced greater surface roughness ($3.61\ \mu\text{m}$). At lower spindle speed (between 690 rpm and 1153 rpm), fiber chip layers were not easily separated from the machining surface. Chip disposal was difficult due to smaller rake and clearance angle of tools. Ineffective machining forces were generated, and material layer separation became complicated when cracks begun to form. This resulted in greater surface irregularities and rougher finishing. Figure 4c shows visible damages, namely rough cutting edges and uncut of fibers when milling with tool-1.

With increased spindle speed from 1153 to 1950 rpm, surface roughness was decreased from 3.46 to $2.41\ \mu\text{m}$ and no visible damages were observed. The outcome is smoother machined surface.

Machining conditions (trial number 21–25 in Table 4) and results are shown in Table 5. Beyond the spindle speeds of 1950 rpm, particularly at 2500 rpm, surface roughness was greatly increased from 2.41 to $3.5\ \mu\text{m}$ pointing to rough machined surface. This is because at higher spindle speeds, high compressive and thrust forces are generated which leads to material deformation and fracture of fibers, indicating greater failures at producing rougher machined surface.

The interaction effect between machining force and surface roughness at five different spindle speeds when milling with tool-1 is shown in Figure 4d.

Higher tangential forces at a higher spindle speed of 2500 rpm resulted in deflecting of cutting tool on the work pieces. Hence, large, segmented chip zones were formed without any uniform chips. Milling surface deteriorated leading to sub-surface damages.

It has been noted higher spindle speeds of 2500 rpm with maximized resultant forces ($34.1\ \text{N}$), low rake and clearance angle of tool-1, did not reduce surface roughness. At maximum spindle speed, high friction was generated which then produced more thermal stresses. It led to tool clogging problem which needed to be addressed by tool plowing on milling surface. Consequently, glass resin and fiber were fractured while the tool rotated toward the rake face of the work piece 4. Greater thrusting resulted in thermo-mechanical action which in turns resulted in friction between tool and work piece interface due to high plowing action of tool on the fibers. This surface roughness ($3.5\ \mu\text{m}$) meant the surface finish was poor. Figure 4e shows smears in glass resin and fracture of fibers.

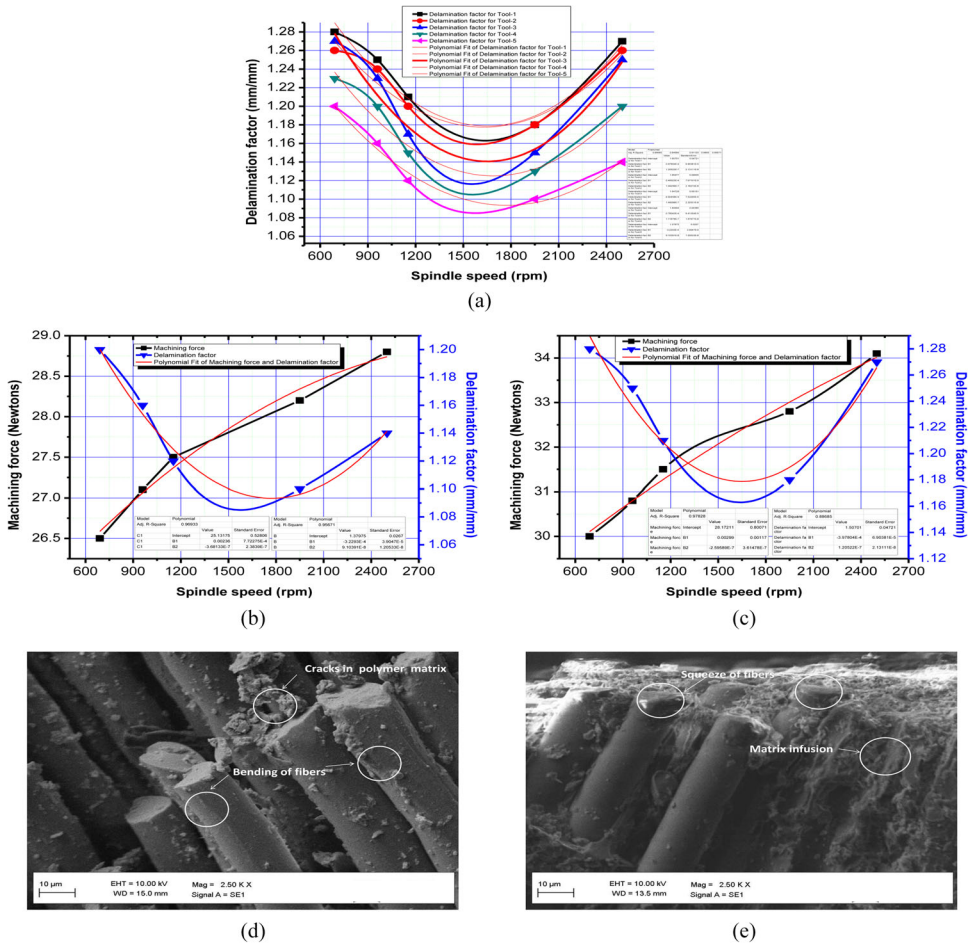


Figure 5. (a) Spindle speed versus delamination factor using five types of tools. (b) The interaction effect of machining force and delamination factor at five spindle speeds with tool-5. (c) The interaction effect of machining force and delamination factor at five spindle speeds with tool-1. (d) SEM image for machined surface damages of GFRP laminate when milling with tool-1 at a spindle speed of 690 rpm. (e) SEM image for machined surface failures of GFRP laminate when milling with tool-1 at a spindle speed of 2500 rpm.

Machining effects on delamination factor

Figure 5a shows the effect of spindle speed on delamination factor using five types of tools.

Figure 5b shows the interaction effect between machining force and delamination factor at five different spindle speeds when milling with tool-5. The effect of spindle speed on delamination factor is described below.

The experimental arrangement is shown in Table 4 (trial number 1 to 20) and its results are shown in Table 5. Calculated delamination factor is decreased from 1.28 to 1.1 considerably when spindle speed was increased from 690 to 1950 rpm. At spindle speed of 1950 rpm, larger rake angle

tool-5 was used with both adjacent vertical wall surface of milling slot resulting in significant cutting action between tool rake face and work piece at aggressive machining forces (28.2 N). At the shortest time of cutting action of tool i.e., if the tool is disengaged from work piece quickly there is a possibility of smoother fiber cuts due to tool rake and clearance angles. Continuous chips were produced in a fine powder form. Hence, no discernible delamination was seen.

The interaction effect between machining force and delamination factor at five different spindle speeds when milling with tool-1 is shown in Figure 5c.

Table 4 shows experimental trial 1 to 5 at lower spindle speed of 690 rpm and lower cutting force at 30 N. This force was inadequate which resulted in uncut fiber passing below tool-1 rake face near matrix material. Here, lesser deformation of fiber was seen. There is therefore matrix withdrawal in the form of segments. Matrix separation was difficult and partial cracking of matrix and bending of fiber was observed. There was peeling of fibers and cracking of matrix which degraded surface quality. Maximized delamination was at 1.21. Damages, such as matrix crack and bending of fibers, are shown in SEM Figure 5d.

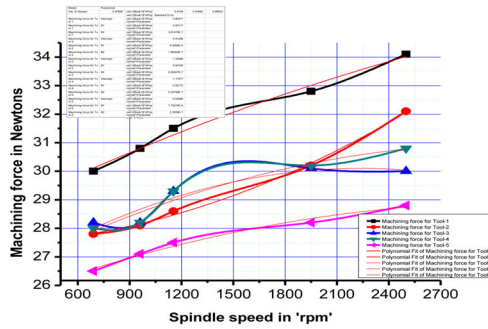
Machining conditions are shown in Table 4 (trial number 21 to 25) and it indicates beyond 1950 rpm i.e., at higher spindle speeds of 2500 rpm using tool-1, the work piece is penetrated rapidly due to high compressive and thrust forces. High friction was created between tool rake face and work piece. The thrusting forces were increased which resulted in shear zone rubbing due to low clearance angle of the tool. Thereby, fibers tended to bend easily and get crushed. It was evident maximum delamination was achieved at 1.27. Figure 5e shows damage mechanisms due to fiber squeezing and matrix infusion.

Machining effects on cutting force

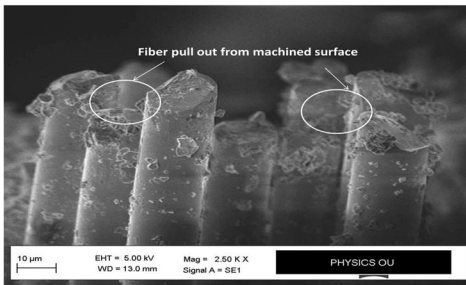
The effect of spindle speed on machining force is described below:

Figure 6a shows the effect of spindle speed on machining force with five different end milling tools. The machining force interaction effect with surface roughness and delamination factor is shown in Figures 4b, d, 5b, and c.

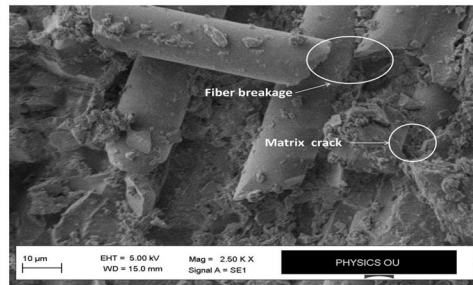
The experimental conditions are shown in Table 4 (trial number 1–20) and their results are shown in Table 5. When spindle speed was increased from 690 rpm to 1950 rpm, the machining force was considerably increased from 30 N to 32.8 N. The measurable outcomes i.e., surface roughness and delamination factor were considerably decreased from 3.61 μm to 2.41 μm



(a)



(b)



(c)

Figure 6. (a) Spindle speed versus machining force using five tools. (b) SEM image for machined surface damages of GFRP laminate when milling with tool-2 at a spindle speed of 690 rpm. (c) SEM image for machined surface damages of GFRP laminate when milling with tool-2 at a spindle speed of 2500 rpm.

and 1.28 to 1.1. Therefore, with increased spindle speeds, the cutting forces were laterally and linearly increased.

When milling with low rake and clearance angle tools (1,2,3, and 4) at low spindle speeds from 690 rpm to 1153 rpm, there was a withdrawal of chips having brush-like fibers with minimum chip thickness. Elastic recovery was difficult and matrix fracture more complex resulting in larger chip segments. The cutting action became complicated, distinctly bulkier chips were formed, tool clogging and complicated chip formation mechanism. There was also fiber pull out and other sub-surface damages. The machined surface became asymmetrical and surface quality deteriorated. Further, machined surface became rougher and delamination was experienced. The failure mechanism is shown in Figure 6b which details failure modes, such as fiber pull out and subsurface damages.

At the optimal spindle speed of 1950 rpm (trials from 16 to 20) and sufficient machining force at 28.2 N milling with tool-5 having larger rake and clearance angle facilitate cutting action and quicker impairing of chips. Therefore, the chips were extracted quickly along the cutting direction. These desirable deformations of continuous chips happened due to less bouncing action of the high clearance angle tool. The material removal rate

was increased and there was no obstruction during extraction of chips from milling surface. Thus, machined surface became smoother at $2.8\ \mu\text{m}$ and delamination factor was less at 1.1.

Milling conditions are shown in [Table 4](#) (trial number 21 to 25). When spindle speed was varied from 1950 rpm to 2500 rpm, the machining forces were drastically increased from 32.8 N to 34.1 N in tool advancement before chips were removed from the milled area.

It was difficult to obtain shear deformation to remove the chips away from the surface at low rake angle tool-1 with increased machining force (34.1 N).

Inter-laminar shear forces were observed at fiber matrix interface due to high compressive machining forces in tool advancement mechanism. Severe damages were seen, namely bending of fibers, bending, matrix cracks and delamination. [Figure 6c](#) shows surface failures, such as matrix crack and fiber breakage.

Conclusion

The current study is focused on the tool performances and effect of input process parameters on milling surface quality of GFRP composite laminates.

1. The cutting mechanism was influenced by spindle speed and tool geometries.
2. The machined surface quality was significantly influenced by tool angles and spindle speeds. The following were noted:
 - Moderate spindle speed of 1950 rpm generated machining force around 23.5 N for improved surface quality.
 - Neither lower spindle speed at 690 rpm nor higher spindle speed at 2500 rpm is recommended for desirable machined surface quality.
 - Higher tool rake angled, and clearance angled tool-5 is recommended for better performance i.e., minimal surface damages.
 - Lower tool rake angled and clearance angled tools (tool-1, 2, 3, and 4) did not provide attractive results.
3. The SEM evaluation based on milling surface quality of GFRP composites at different phases are described below.
 - Milling conditions of spindle speed at 1950 rpm, feed rate 120 mm/min, and depth of cut 3 mm with tool-5 helped to avoid thermo-mechanical failures and minimized machined surface damages.
 - More surface damages were noted, when milling with low rake and clearance angled tools (tool-1, 2, 3, and 4).

4. Varying of other factors, such as work piece characteristics (fiber volume fraction, fiber ply orientation, properties of work piece material) and conditions may be influenced results related to desirable machined surface quality.
5. Further investigations in these directions could lead to established ISO standardization.

Nomenclature

GFRP	glass fiber reinforced polymer
FRP	fiber reinforced polymer
CFRP	carbon fiber reinforced polymer
SMC	sheet mold compound
CVD	chemical vapor deposition
PVD	physical vapor deposition
F_x	feed force
F_y	cutting force
F_z	thrust force
F_R	resultant force
F_m	machining force
R_a	surface roughness
F_D	delamination factor
W_{Max}	width of the slot after machining in mm
W	actual width of the slot in mm

ORCID

Chandra Mouli Badiganti  <http://orcid.org/0000-0002-8213-6555>

References

- Abrão, A.M.; Faria, P.E.; Rubio, J.C.C.; Reis, P.; Davim, J.P. (2007) Drilling of fiber reinforced plastics: A review. *Journal of Materials Processing Technology*, 186(1–3): 1–7. doi: [10.1016/j.jmatprotec.2006.11.146](https://doi.org/10.1016/j.jmatprotec.2006.11.146)
- An, Q.; Cai, C.; Cai, X.; Chen, M. (2019) Experimental investigation on the cutting mechanism and surface generation in orthogonal cutting of UD-CFRP laminates. *Composite Structures*, 230: 111441. doi:[10.1016/j.compstruct.2019.111441](https://doi.org/10.1016/j.compstruct.2019.111441)
- An, Q.; Chen, J.; Ming, W.; Chen, M. (2021) Machining of SiC ceramic matrix composites: A review. *Chinese Journal of Aeronautics*, 34(4): 540–567. doi:[10.1016/j.cja.2020.08.001](https://doi.org/10.1016/j.cja.2020.08.001)
- An, Q.; Dang, J.; Li, J.; Wang, C.; Chen, M. (2020) Investigation on the cutting responses of CFRP/Ti stacks: With special emphasis on the effects of drilling sequences. *Composite Structures*, 253(May): 112794. doi:[10.1016/j.compstruct.2020.112794](https://doi.org/10.1016/j.compstruct.2020.112794)
- An, Q.; Ming, W.; Cai, X.; Chen, M. (2015) Effects of tool parameters on cutting force in orthogonal machining of T700/LT03A unidirectional carbon fiber reinforced polymer laminates. *Journal of Reinforced Plastics and Composites*, 34(7): 591–602. doi:[10.1177/0731684415577688](https://doi.org/10.1177/0731684415577688)
- Arola, D.; Ramulu, M. (1997) Orthogonal cutting of fiber-reinforced composites: A finite element analysis. *International Journal of Mechanical Sciences*, 39(5): 597–613. doi:[10.1016/S0020-7403\(96\)00061-6](https://doi.org/10.1016/S0020-7403(96)00061-6)

- Arola, D.; Ramulu, M.; Wang, D.H. (1996) Chip formation in orthogonal trimming of graphite/epoxy composite. *Composites Part A: Applied Science and Manufacturing*, 27(2): 121–133. doi:10.1016/1359-835X(95)00013-R
- Azmi, A.I.; Lin, R.J.T.; Bhattacharyya, D. (2012) Experimental study of machinability of GFRP composites by end milling. *Materials and Manufacturing Processes*, 27(10): 1045–1050. doi:10.1080/10426914.2012.677917
- Cai, X.; Zhou, R.; Shen, L.; Tang, H.; An, Q. (2019) An experimental investigation on precision machining mechanism of carbon fibre reinforced polymer. *International Journal of Abrasive Technology*, 9(1): 16–30. doi:10.1504/IJAT.2019.097965
- Calzada, K.A.; Kapoor, S.G.; Devor, R.E.; Samuel, J.; Srivastava, A.K. (2012) Modeling and interpretation of fiber orientation-based failure mechanisms in machining of carbon fiber-reinforced polymer composites. *Journal of Manufacturing Processes*, 14(2): 141–149. doi:10.1016/j.jmapro.2011.09.005
- Can, A. (2019) Study on the machinability of SMC composites during hole milling: Influence of tool geometry and machining parameters. *Arabian Journal for Science and Engineering*, 44(9): 7599–7616. doi:10.1007/s13369-019-03865-z
- Chatelain, J.F.; Zaghbani, I. (2012) A comparison of special helical cutter geometries based on cutting forces for the trimming of CFRP laminates. *International Journal of Mechanics*, 6(1): 52–59.
- Davim, J.P.; Reis, P. (2005) Damage and dimensional precision on milling carbon fiber-reinforced plastics using design experiments. *Journal of Materials Processing Technology*, 160(2): 160–167. doi:10.1016/j.jmatprotec.2004.06.003
- Giasin, K.; Gorey, G.; Byrne, C.; Sinke, J.; Brousseau, E. (2019) Effect of machining parameters and cutting tool coating on hole quality in dry drilling of fibre metal laminates. *Composite Structures*, 212(15): 159–174. doi:10.1016/j.compstruct.2019.01.023
- Iliescu, D.; Gehin, D.; Iordanoff, I.; Girot, F.; Gutiérrez, M.E. (2010) A discrete element method for the simulation of CFRP cutting. *Composites Science and Technology*, 70(1): 73–80. doi:10.1016/j.compscitech.2009.09.007
- Jahromi, A.S.; Bahr, B.; Krishnan, K. (2014) An analytical method for predicting damage zone in orthogonal machining of unidirectional composites. *Journal of Composite Materials*, 48(27): 3355–3365. doi:10.1177/0021998313509862
- Langari, J.; Kolahan, F.; Aliakbari, K. (2016) Effect of tool speed on axial force, mechanical properties and weld morphology of friction stir welded joints of A7075-T651. *International Journal of Engineering*, 29(3): 403–410. doi:10.5829/idosi.ije.2016.29.03c.15
- Latha, B.; Senthilkumar, V.S.; Palanikumar, K. (2011) Modeling and optimization of process parameters for delamination in drilling glass fiber reinforced plastic (GFRP) composites. *Machining Science and Technology*, 15(2): 172–191. doi:10.1080/10910344.2011.579802
- Lopresto, V.; Caggiano, A.; Teti, R. (2016) High performance cutting of fibre reinforced plastic composite materials. *Procedia CIRP*, 46: 71–82. doi:10.1016/j.procir.2016.05.079
- Ming, I.W.M.; Azmi, A.I.; Chuan, L.C.; Mansor, A.F. (2018) Experimental study and empirical analyses of abrasive waterjet machining for hybrid carbon/glass fiber-reinforced composites for improved surface quality. *The International Journal of Advanced Manufacturing Technology*, 95(9–12): 3809–3822. doi:10.1007/s00170-017-1465-9
- Palanikumar, K. (2007) Modeling and analysis for surface roughness in machining glass fibre reinforced plastics using response surface methodology. *Materials & Design*, 28(10): 2611–2618. doi:10.1016/j.matdes.2006.10.001
- Prasanth, I.S.N.V.R.; Ravishankar, D.V.; Hussain, M.M. (2017a) Comparative evaluation on milled surface quality of GFRP composites by different end mill tools. *International*

- Journal of Machining and Machinability of Materials*, 19(5): 483–504. doi:10.1504/IJMMM.2017.087622
- Prasanth, I.S.N.V.R.; Ravishankar, D.V.; Hussain, M.M.; Badiganti, C.M.; Sharma, V.K.; Pathak, S. (2018) Investigations on performance characteristics of GFRP composites in milling. *The International Journal of Advanced Manufacturing Technology*, 99(5–8): 1351–1360. doi:10.1007/s00170-018-2544-2
- Prasanth, I.S.N.V.R.; Ravishankar, D.V.; Hussain, M.M. (2017b) Analysis of milling process parameters and their influence on glass fiber reinforced polymer composites. *IJE TRANSACTIONS A: Basics*, 30(7): 1074–1080. [10.5829/ije.2017.30.07a.17](https://doi.org/10.5829/ije.2017.30.07a.17)
- Prashanth, I.S.N.V.R.; Ravi Shankar, D.V.; Manzoor Hussain, M.; Chandra Mouli, B. (2018) Critical analysis in milling of GFRP composites by various end mill tools. *Materials Today: Proceedings*, 5(6): 14607–14617. doi:10.1016/j.matpr.2018.03.052
- Ramulu, M. (1997) Machining and surface integrity of fibre-reinforced plastic composites. *Sadhana*, 22(3): 449–472. doi:10.1007/BF02744483
- Shojaeefard, M.H.; Khalkhali, A.; Shahbaz, S.O. (2019) Low-carbon steel sheet asymmetric single-point incremental forming: Analysis and optimization of the surface roughness. *International Journal of Engineering, Transactions C: Aspects*, 32(6): 866–871. [10.5829/ije.2019.32.06c.10](https://doi.org/10.5829/ije.2019.32.06c.10)
- Slamani, M.; Chatelain, J.F.; Hamedanianpour, H. (2019) Influence of machining parameters on surface quality during high speed edge trimming of carbon fiber reinforced polymers. *International Journal of Material Forming*, 12(3): 331–353. doi:10.1007/s12289-018-1419-2
- Slamani, M.; Gauthier, S.; Chatelain, J.F. (2015) A study of the combined effects of machining parameters on cutting force components during high speed robotic trimming of CFRPs. *Measurement*, 59: 268–283. doi:10.1016/j.measurement.2014.09.052
- Srinivasan, T.; Palanikumar, K.; Rajagopal, K.; Latha, B. (2017) Optimization of delamination factor in drilling GFR-polypropylene composites. *Materials and Manufacturing Processes*, 32(2): 226–233. doi:10.1080/10426914.2016.1151038
- Wang, D.H.; Ramulu, M.; Arola, D. (1995) Orthogonal cutting mechanisms of graphite/epoxy composite. Part I: Unidirectional laminate. *International Journal of Machine Tools and Manufacture*, 35(12): 1623–1638. [https://doi.org/10.1016/0890-6955\(95\)00014-O](https://doi.org/10.1016/0890-6955(95)00014-O) doi:10.1016/0890-6955(95)00014-O
- Zhang, L.C.; Zhang, H.J.; Wang, X.M. (2001) A force prediction model for cutting unidirectional fibre-reinforced plastics. *Machining Science and Technology*, 5(3): 293–305. doi:10.1081/MST-100108616